Publishing Excellence Inspiring Progress
ARISTON PUBLICATIONS
Energy & Environment Advances
ISSN: 3066-5728 https://aristonpubs.com/energy-environment-advances https://doi.org/10.69626/eea.2025.0010

RESEARCH ARTICLE

Synthesis and Electrochemical Evaluation of CuO/ZnO @Hierarchical Porous Graphitic Carbon Spheres for Enhanced Supercapacitive Applications

Afia Asghar [1], Saima Anjum [1,*], Nishat Fatima [1], Muhammad Imran Khan [2,*], Abdallah Shanableh [2,3]

ABSTRACT: In this study, CuO/ZnO@hierarchical porous graphitic carbon spheres (CuO/ZnO@HPGCS) nanocomposites were synthesized via a cost-effective low-temperature water-bath technique. Chitosan was employed as a carbon precursor, while PVP and PEG acted as stabilizing agents to ensure the formation of well-structured porous carbon spheres. Comprehensive characterization techniques, including scanning electron microscopy (SEM), X-ray diffraction (XRD), and energy-dispersive X-ray spectroscopy (EDX), were utilized to analyze the morphology, structure, and elemental composition of the synthesized materials. The electrochemical behavior of the CuO/ZnO@HPGCS electrodes was evaluated using cyclic voltammetry (CV), galvanostatic charge-discharge (GCD), and electrochemical impedance spectroscopy (EIS). Compared to pure CuO/ZnO and standalone HPGCS electrodes, the CuO/ZnO@HPGCS nanocomposites exhibited significantly improved supercapacitive performance. The specific capacitance of CuO/ZnO@HPGCS reached an impressive 1875 F/g at a scan rate of 10 mV/s, substantially outperforming CuO/ZnO (1229 F/g) and HPGCS (798 F/g). This enhancement can be attributed to the synergistic effect between the high conductivity and large surface area of HPGCS and the electroactive properties of transition metal oxides. The porous structure of HPGCS provided ample active sites and improved charge transfer dynamics, thereby boosting the overall electrochemical performance. The study demonstrates the potential of CuO/ZnO@HPGCS nanocomposites as advanced materials for energy storage applications, offering a scalable and cost-efficient approach to fabricating high-performance supercapacitor electrodes for industrial and commercial use.

Keywords: Nanocomposites, Supercapacitors, Energy storage, Transition metal oxides, Carbon spheres.

Received: 13 August 2024; Revised: 15 October 2024; Accepted: 03 December 2024; Published Online: 11 January 2025

1. INTRODUCTION

In this modern era of technology, the global demand for energy has significantly increased. There is a significant role of energy in our daily life as well as in our social and economic development as the modern world economy is totally dependent upon the reliable energy sources [1]. Presently, fossil fuels, derived from coal and petroleum, remain the primary source of energy. However, overreliance on these fossil-based fuels has had dual consequences [2]. Fossil fuel scarcity, in addition to adverse environmental impacts and hazardous chemical discharge, places a substantial burden on human society [3]. So there is an urgent need to paying attention on clean, sustainable and inexhaustible energy commodities, comprising sun propulsion, tidal power and wind energy [4,5].

To validate a long-term durability and uninterrupted energy conversion and transmission, the energy harvesting technology must be synchronized with viable, affordable, and secure electroactive material. In the present world, the

[1] Department of Chemistry, Govt. Sadiq College Women University, Bahawalpur, Pakistan.
[2] Research Institute of Sciences and Engineering (RISE), University of Sharjah, Sharjah 27272, United Arab Emirates.
[3] Scientific Research Center, Australian University, Kuwait.

* Author to whom correspondence should be addressed:
drsaima@gscwu.edu.pk (Saima Anjum)
raoimranishaq@gmail.com (Muhammad Imran Khan)

© Ariston Publications 2025. All rights reserved.

storage of electrical energy generated from various sources plays a critical role for sustainable growth. In the sectors of portable electronics and transportation, the realem of electrochemical energy storage has witnessed significant growth, driven by advancement in electrochemical capacitors and cutting edge battery technology [6].

Compared to traditional batteries, supercapacitors offer higher power densities, lower discharge rates, higher energy densities, and extended cycle lives [7]. The overall notable advancement in supercapacitor functionality influenced by substance used for the electrodes. Thus, the production of critical electrode specie with remarkable potential is one of the crucial step [8]. Supercapacitor taxonomy reveals three discrete types, each categorized by unique electrode substrate and charge storage mechanism which are i) electric double-layer capacitor, ii) pseudocapacitor and iii) hybrid capacitor [9]. In EDLC the electrochemically active surface are primarily composed up of carbon material which stores energy by surface assimilation between electrode and electrolyte. There are no any faradic reactions occurring in this type of capacitor. In second type of capacitor the transition metal oxides are used and the charge reserve through redox reaction. While the hybrid capacitor merge the materials used in both the EDLC and pseudocapacitors, reserving the energy through the assimilation of electrostatic charge adsorption and oxidation-reduction reaction [8,10].

Transition metal oxides (TMOs) demonstrate improved mechanical strength and increase efficiency for supercapacitors as a consequence of their good electrical conductivity and good capacitance value as well as easy availability and environmental friendliness but a significant limitation of TMOs is their relatively lower charge density [11,12]. On the other hand, the conducting polymers, like carbon-based materials, are also considered as superior electrode materials in consequence of their low manufacturing cost, superior electron transfer mobility, environmental friendliness, and optimized mechanical strength. Among these, activated carbon (AC) is one of the most popular capacitive material with superior capacitive properties and reasonable porous structures [13,14]. When it comes to ion diffusion in devices, the presence of a porous material exhibit decisive effects. . Furthermore, the presence of porosity will facilitate improved electrolyte penetration, enhancing the prevalence of electrochemical interfaces and thereby improving the capacitive performance [15].

To overcome various limitations of TMO and carbon structure (lower cyclic stability), both the material are often combined together as TMO/carbon material with enhanced electrical conductivity, high capacitance, as well as high power density and energy density[16]. Among transition metal oxides; ZnO stands out due to its unique combination of electronic and optical properties making it suitable material for widespread adoption. CuO, an abundant p-type semiconductor, features a small HOMO-LUMO gap, good chemical stability, antiferromagnetic properties, and low cost. For a variety of uses, including supercapacitors, it is regarded as an efficient electrode material [17-23].

Bishwakarma et, al. carried out a detailed analysis of the electrochemical behaviour of composite material formed by mixing n-type ZnO and p-type CuO material exhibiting ambipolar conduction with differing band energies. The resultant flower-shaped structure showed elevated specific capacitance of 313 F/g at a current density of 2 A/g, with 84.1% long term capacitance stability after 5000 cycles [18]. BaQais, A. et al explored the CuO-ZnO in different ratios to check out the capacitive behavior of nanocomposite. Using the ultrasonication method for the preparation and CV and EIS for electrochemical characterization, they found out the highest specific capacitance was obtained for CuO+15% ZnO as 352 F/g under imposed current loading of 1A/g [19].

When carbon-based material exhibiting electric double-layer capacitance (EDLC) is combined with copper(II) oxide (CuO) and zinc oxide (ZnO), both of which possesses the pseudocapacitive properties, a hybrid material is created that integrates both faradaic and non-faradaic properties. This hybrid composite's enhanced electrochemical properties make it suitable for applications in energy storage and charging systems [17]. Fuwang Wen et al. investigated Zn ion hybrid with hierarchical micro perforated carbon material as surface modified redox active material with enhanced electrochemical behavior. This composite shows an excellent capacitance of 301 F/G at 0.1 A/g with high performance retention proficiency [20].

The Cu-doped porous carbon is also investigated as a supercapacitive material by Zhang ET. al. utilizing bamboo biomass as the carbon precursor and employing in-situ polymerization of polypyrrole to enhance disorder and material wettability. These findings demonstrate the promising potential of biomass-originated carbon based molecular structure for supercapacitor technologies, evident in their notable capacitive performance of 508.50 F/g at 0.5 A/g [21]. In another study, biomass was similarly used as a carbon structure source for the synthesis of composites with varying oxide sources, namely ZnO@biomass and CuO@biomass [15].

Herein, we employed a primitive, scalable and affordable production technique to synthesize CuO/ZnO@HPGCSs for high performance supercapacitve applications. The carbon spheres were fabricated using the chitosan/PEG blend as raw materials followed by the growth of CuO/ZnO nanoparticles on it using water bath method. Because of possessing multiscale porosity and increased surface to volume ratio, the produced nanomaterials demonstrated outstanding electrochemical performance in alkaline media. These findings suggested that the fabricated nanomaterials are innovative electrode material for high performance Supercapacitor implementation

2. EXPERIMENTAL DETAILS

2.1. Materials

Analytical reagent grade chemicals were used throughout the research and consumed without subsequent purification.

 © Ariston Publications 2024. All rights reserved

Chitosan, polyethylene glycol-4000, potassium hydroxide, polyvinylpyrrolidone and potassium ferricyanide were purchased from Daejung Chemicals and Metals Co, LTD Korea. Hydrochloric acid, acetic acid, nitric acid, urea and ethanol were of analytical grade. Graphite powder and polyvinylidene fluoride was supplied by sigma Aldrich. All experiments were performed by deionized water.

2.2. Preparation of HPGCS

Solution was prepared by dissolving 6 grams total having 60 % chitosan and 40 % PEG in 100 ml of 2 % acetic acid solution in deionized water. The solution was heated at 50ºC for 1.5 hours with magnetic stirring to get homogenized solution. PVP solution was produced by combining 0.5g PVP in 40ml ethanol and 5ml deionized water and added drop wise into solution while maintaining continue stirring and heating. Potassium ferricyanide solution preparation involved dissolving 1g of $C_6N_6FeK_3$ in 50 ml distilled water and incorporated to the above prepared solution while maintain continuous stirring and heating. After 1.5 hours the solution was cooled down and sonicated to get homogenized solution. Subsequently the solution was dehydrated at 100ºC overnight in a temperature control vacuum oven.

After drying, the sample was grinded to get powdered form and then carbonized at 800ºC for 3 hours. Further the sample was treated with 1M HNO_3 at 80ºC for 1.5 hours to remove the iron compounds. The sample was washed till the pH maintained at 7 and the sample was dehydrated at 100ºC overnight. Then the prepared sample was activated by blending it with KOH in 1:3 with a small amount of water. The blended material was dehydrated in microwave oven and was again carbonized at 800ºC for 3 hours and cooled down naturally. The sample was washed with 1M KOH and distilled water. Then it was dehydrated at 60ºC overnight in temperature control vacuum oven to obtain HPGCS.

2.3. Preparation of CuO/ZnO@HPGCS

CuO/ZnO@HPGCS nanocomposites were fabricated by using an efficient thermo regulated bath procedure. In the formation of composite the equal amount of copper acetate, zinc acetate and the HPGCS were used. 0.0438g zinc acetate salt were taken and dissolved into 50ml ethanol while violently stirring. 0.0438g of Cu acetate were taken and dissolved into ethanol maintaining homogenous stirring until dissolved. Then the solutions of both salts (Cu acetate and Zn acetate) were mixed together while maintaining continuous stirring as a solution A. Prepared HPGCS were dissolved into 30 ml ethanol and the solution were stirred until the HPGCS were dispersed (B).

Then the dispersed solution of HPGCS (B) was continuously added drop wise into salts homogenous solution A to acquire mixture C while sustaining the water bath conditions at 60 ^{0}C for 1h. Then 0.6g of NaOH into 50ml ethanol were taken and added drop wise into previous mixture at a temperature of 60 ^{0}C while maintaining water bath conditions with continuous stirring of 2hs. The resulting product was centrifuged. The CuO/ZnO@ HPGCS were washed three times with ethanol and deionized water. After washing product was vacuum dried at 60 ^{0}C overnight in a vacuum oven.

2.4. Preparation of Ni-foam electrode

The synthesized material was combined in a weight percent ratio of 80:10:10 with electrically conductive carbon material (graphite) and the binding agent polyvinylidene fluoride (PVDF) to create the working electrode. It was then ground, and ethanol was added in to it drop by drop to create homogeneous slurry. After coating the electrode with this slurry, the electrode dehydrated in a temperature control oven for 6 h at 60^{0}C. The 3.0 M KOH aqueous solution, which serves as the alkaline electrolyte, was created. Using the three electrode cell system, electrochemical impedance spectroscopy (EIS) and cyclic voltammetry (CV) were used to test the changed electrodes' electrochemical parameters.

2.5. Instrumentation

Ultraviolet-vis (UV-Vis) spectra were recorded on BMS Biotechnology medical services K Canada INC UV-1602 spectrophotometer. The qualitative structure analysis was done by FTIR Instrument. The configuration and chemical environment of samples were recorded by electron microscope (SEM) and energy dispersive X-ray spectroscopy (EDX) system. The crystal molecular configuration of the sample were elucidated by powder X-ray diffraction (XRD) patterns using X-ray diffractometer with Cu Kα (λ=1.5418 Å) as the source. Cyclic voltammetry measurements were performed on CHI 660C potentiostat (CH Instruments, Origaflex-OGF-Multichannels-OrigaLys) at room temperature. All electrochemical evaluations were carried out in 3M KOH with institutionalized three electrode system corresponding silver electrode as reference electrode, nickel foam electrode as working electrode and Pt wire as counter electrode.

3. RESULTS AND DISCUSSION

3.1. SEM and EDX

The surface morphology and elemental composition of HPGCS and CuO/ZnO@HPGCS were thoroughly examined using scanning electron microscopy (SEM) and energy-dispersive X-ray spectroscopy (EDX). SEM was employed at various magnifications to analyze the structural features and surface characteristics of the synthesized materials. Figures 1 (a, b, c) illustrate the SEM images of HPGCS, while Figures 1 (d, e, f) depict the SEM images of CuO/ZnO@HPGCS.

© Ariston Publications 2025. All rights reserved.

The SEM images of HPGCS revealed spherical carbon particles with an average diameter of approximately 34 nm. The spheres exhibited a relatively smooth surface texture interspersed with fiber-like structures, likely attributed to the catalytic graphitization effect during the carbonization process. Notably, the porous structure of the HPGCS was evident, which facilitates the penetration of electrolytes into the aggregates, creating three-dimensional channels that enhance ion transport.

For the CuO/ZnO@HPGCS nanocomposite, the SEM images showed a well-integrated three-dimensional mesoporous network. The inclusion of CuO and ZnO nanoparticles within the carbon matrix not only preserved the porosity but also provided additional interfaces for ion permeation. These mesoporous architectures are critical for improving the electrochemical performance of the material by enabling efficient charge storage and rapid ion diffusion.

The EDX analysis further confirmed the elemental composition of the synthesized materials. The spectrum indicated the presence of carbon, oxygen, copper, and zinc in the CuO/ZnO@HPGCS nanocomposite, with no detectable impurities. This verifies the successful incorporation of CuO and ZnO into the hierarchical porous graphitic carbon spheres. The quantitative composition ratios of the elements, as depicted in Figures 1 (g, h), support the homogeneity and purity of the synthesized composite. The synergy between the carbon spheres and metal oxides is pivotal in achieving the enhanced performance observed in the subsequent electrochemical studies.

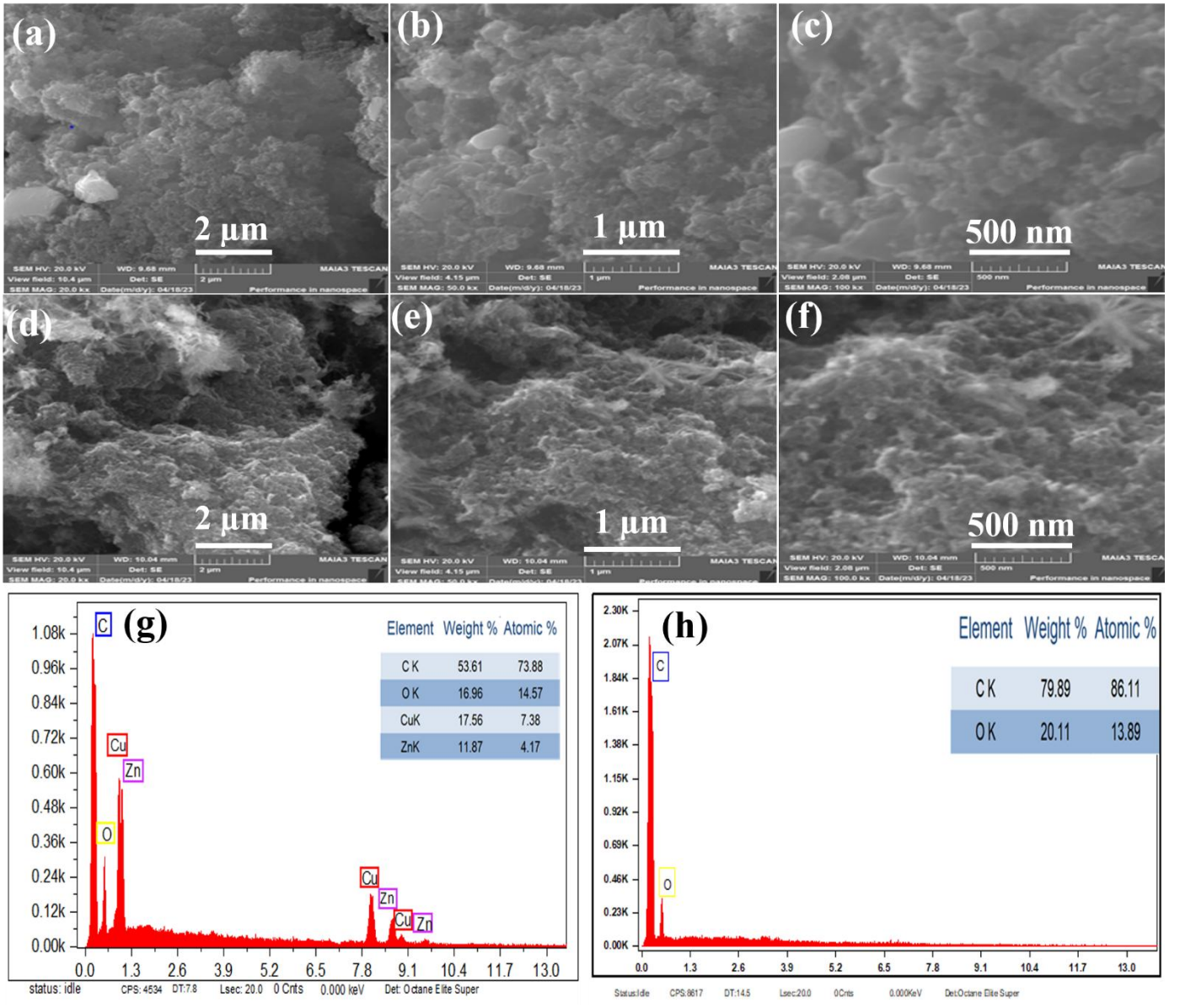


Fig. 1. SEM images of (a-c) SEM images for HPGCS, and (d-f) CuO/ZnO@HPGCS. EDX spectra for (g) HPGCS, and (b) CuO/ZnO@HPGCS.

 © Ariston Publications 2024. All rights reserved

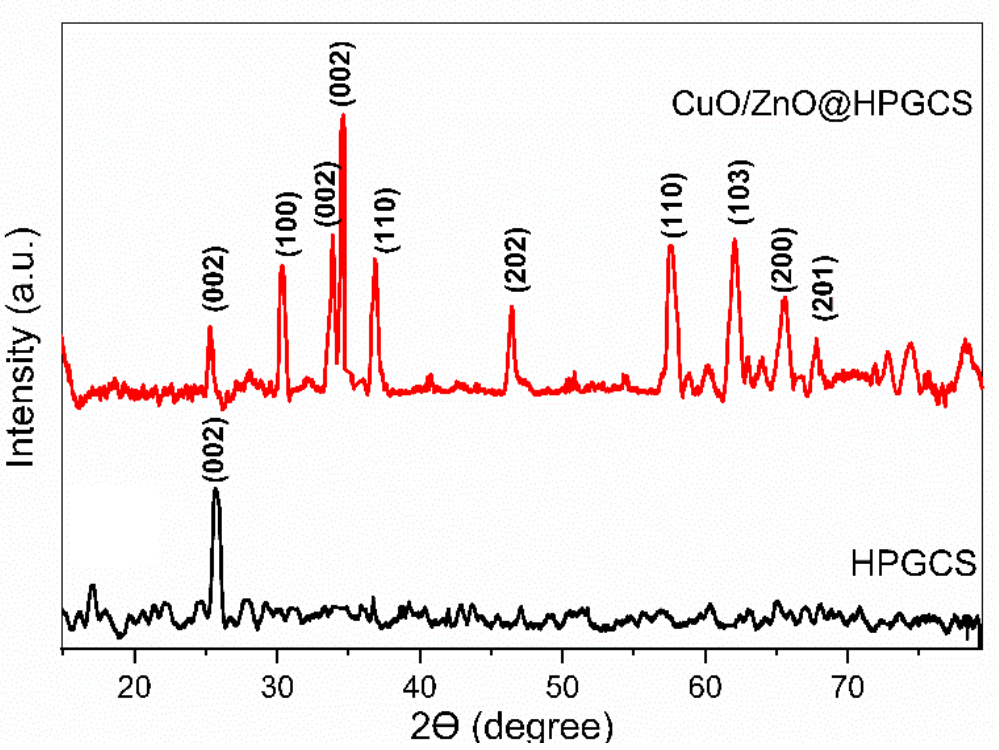


Fig. 2. XRD pattern of CuO/ZnO@HPGCS.

3.2. X-ray diffraction

For the confirmation of the graphitized structure of doped carbon in CuO/ZnO, CuO/ZnO@HPGCS analyzed by XRD. The XRD pattern of doped carbon in Figure 2 showed the diffraction peaks at 2θ around 25º, indexed to (002) crystallographic planes. XRD spectra revealed that highly graphitic structure was developed by catalytic graphitization by the potassium ferricyannide. The (002) peak indicates the graphitic structure formation [22]. The detected values are consistent with the incorporation of graphitic layers within the spherical carbon nanostructure. The crystallite size calculated from peak (002) was found to be 16.13 nm. All of the peaks of the CuO/ZnO@HPGCS indicated the presence of high purity CuO/ZnO as peaks can be seen at 2θ value =33.4°, 35.6°, 37.91°,48.05°, 58.4°, 60.9°, 62.8° and 66.22° corresponding to the spinel nickel cobaltite phase with the plane reflection from (100), (002), (101), (111), (102), (110), (103), (112) and (201) which agree well with the spinel phase of CuO/ZnO [23]. The peaks at 26.3° is the characteristic peak of carbon nanospheres in CuO/ZnO@HPGCS the confirmed its presence. No impurity peaks were seen. The crystallite size calculated from peak (101) was found to be 15.81 nm.

3.3. FTIR spectra analysis

Figure 3 presents the Fourier-transform infrared (FTIR) absorption spectra of HPGCS, CuO/ZnO, and CuO/ZnO@HPGCS, offering insights into their chemical composition and functional groups. The analysis highlights distinct absorption peaks corresponding to various vibrational modes, confirming the presence of characteristic bonds and chemical functionalities within the materials. The broad absorption band observed in the range of 3100–3500 cm^{-1} corresponds to O–H stretching vibrations, indicating the presence of hydroxyl groups. This peak is typically associated with adsorbed water molecules or surface hydroxyl groups, which contribute to the hydrophilicity of the materials. A sharp peak at 2661 cm^{-1} corresponds to C–H stretching vibrations, characteristic of alkyl groups. The absorption band at 2312 cm^{-1} is attributed to O=C=O stretching vibrations, which are indicative of carbonyl functional groups. Similarly, a peak at 2100 cm^{-1} corresponds to C≡N stretching vibrations, confirming the presence of nitrile groups within the material matrix. The bending vibrations of C–H bonds are observed at 1917 cm^{-1}, while a prominent peak at 1743 cm^{-1} corresponds to the stretching vibrations of C=O bonds, which are characteristic of ester or ketone groups. In the fingerprint region, the C=C stretching vibrations are evident at 1045 cm^{-1}, while the bending vibrations of C=C bonds are confirmed by the absorption band at 787 cm^{-1}. Additionally, the C–N stretching vibration bands are observed at 1333 cm^{-1}, indicating the presence of amine or related functional groups. The low-frequency region, between 400–750 cm^{-1}, reveals distinct peaks associated with the presence of CuO and ZnO within the composite structure.

© Ariston Publications 2025. All rights reserved.

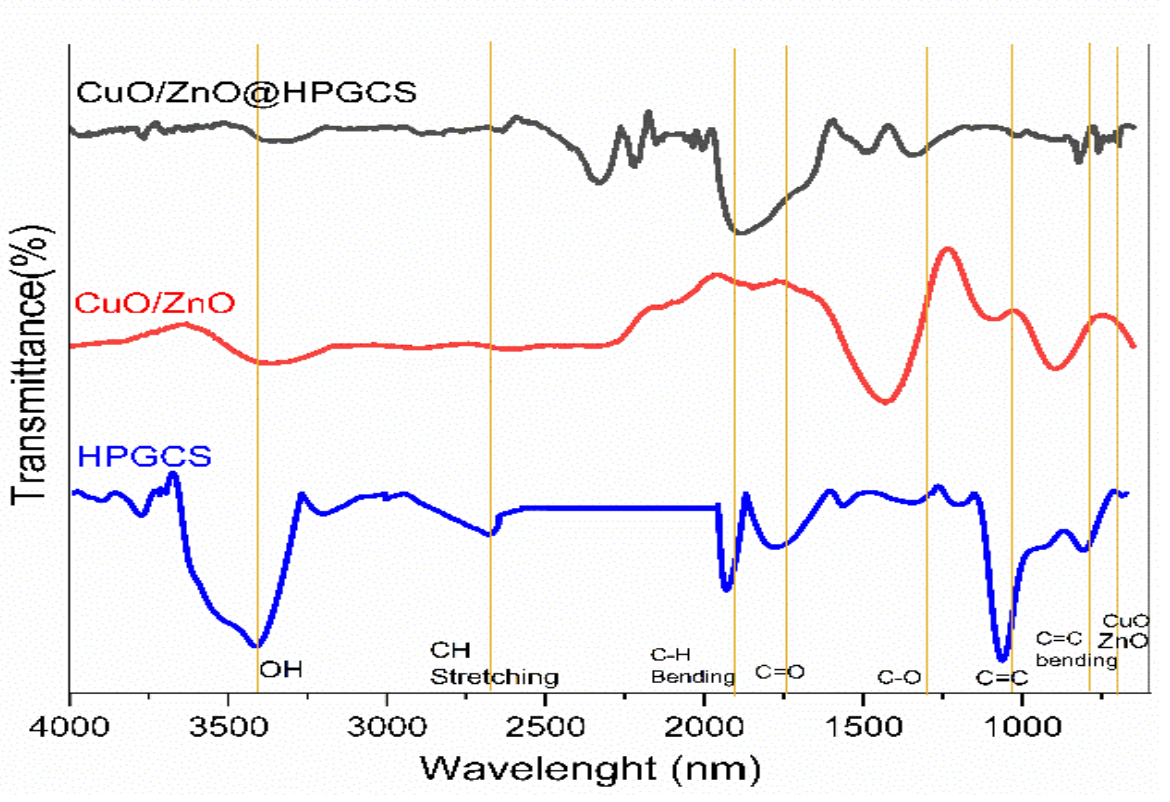


Fig. 3. FTIR spectra of HPGCS, CuO/ZnO and CuO/ZnO@HPGCS materials.

These metal–oxygen stretching vibrations confirm the successful integration of CuO and ZnO nanoparticles in both CuO/ZnO and CuO/ZnO@HPGCS samples. The FTIR analysis demonstrates the coexistence of organic and inorganic components in CuO/ZnO@HPGCS, validating the hybrid nature of the composite. The observed functional groups, particularly the O–H, C–H, and C=O bonds, along with the CuO and ZnO signatures, highlight the composite's potential for enhanced electrochemical performance and compatibility in energy storage applications.

3.4. Electrochemical performance

The three-electrode system was used to study the prepared nanocomposites. The active material functioned as the working electrode, following its successful deposition on the Ni foam, Ag/AgCl electrode was employed as reference electrode, and platinum (Pt) wire as a counter electrode for all electrochemal experiment. The electrochemical cell was filled with 3.0 M KOH electrolyte solution, which provide a high ionic conductivity.

3.4.1. Cyclic voltammetry

The HPGCS, CuO/ZnO and CuO/ZnO@HPGCS was estimated as electrode material for supercapacitor applications by using 3M KOH electrolyte. The voltage window was chosen using CV at scan rate of 10mV/s for values between -0.2 and +0.9 for CuO/ZnO@HPGCS and between -0.3 and +0.9for CuO/ZnO.

In case of HPGCS, the potential window was chosen at 10 mV/s using cyclic voltammetry for values from -0.1 to +0.8. The CV was carried out atscan rates ranging from 10 to 100 mV/s. Figure 4(a) showed a typical voltammogram for HPGCS at various scan rates. Even at higher scan rates, forms of CV curves were well retained, demonstrating excellent capacitive behavior. Specific capacitance was estimated at different scan rates and a decline in specific capacitance was observed with rise in scan rates. This is because of ionic and electrical transport, but Cs of carbon nanospheres was kept relatively constant at higher scan rates, showed that this material exhibited good high-current capacitive behavior. The appropriate mesopores size distribution on the carbon nanospheres, that provides adequate availability for electrolyte even at greater current, is likely responsible for this exceptional high-current capacitive performance. High capacitance retention at fast current density or high scan rate is a critical property of capacitor electrodes as a result of the practical applications of supercapacitors that need high current densities for charging and discharging.

In case of CuO/ZnO without the incorporation of mesoporous carbon spheres, the CV was run at various scan rates ranging from 10 and 100 mV/s. The voltage window was determined using CV at scan rate of 10mV/s, with values

 © Ariston Publications 2024. All rights reserved

between -0.3 and +0.9V for CuO/ZnO. Figure 4 (b) showed a typical voltammogram for CuO/ZnO at various scan rates. The CV curves' form was well preserved even at higher scan rates, demonstrating excellent capacitive behaviour. The specific capacitance calculation were performed at multiple scan rates, revealing a decrease in specific capacitance with the increase in the scan rates.

In case of CuO/ZnO@HPGCS, the cyclic voltammetry was performed at various scan rates, ranging from 10 to 100 mV/s. Figure 4 (c) showed a typical voltammogram for CuO/ZnO@HPGCS at various scan rates. Even at higher scan rates, the CV curves' appearance was well retained, demonstrating excellent capacitive behavior. The specific capacitance values were performed at multiple scan rates, revealed that as the scan rates increased, a decline in the particular capacitance was seen. This is because of electrical and ionic transport, but the specific capacitance was kept relatively constant at higher scan rates, showed that this material exhibited good high-current capacitive performance. The incorporation of carbon spheres provided good accessibility for electrolyte even at very high currents which contributed to the exceptional high-current capacitive performance of the sample. Its capacitance was much greater as compared to those of CuO/ZnO as the addition of carbonaceous material improved overall capacitance.

3.4.2. Electrochemical impedance spectroscopy

An extremely strong method called electrochemical impedance spectroscopy was used to examine electronic and electrochemical reactions of electrode material (EIS). The Nyquist sequences were conducted in a three-electrode setup at the open circuit potential. Figure 5(A) displays the sample's Nyquist plot at frequencies between 0.01 Hz and 100 kHz. For the CuO/ZnO@HPGCS composite, the high frequency area of the Nyquist plot did not exhibited a semicircle demonstrating good supercapacitive behavior.

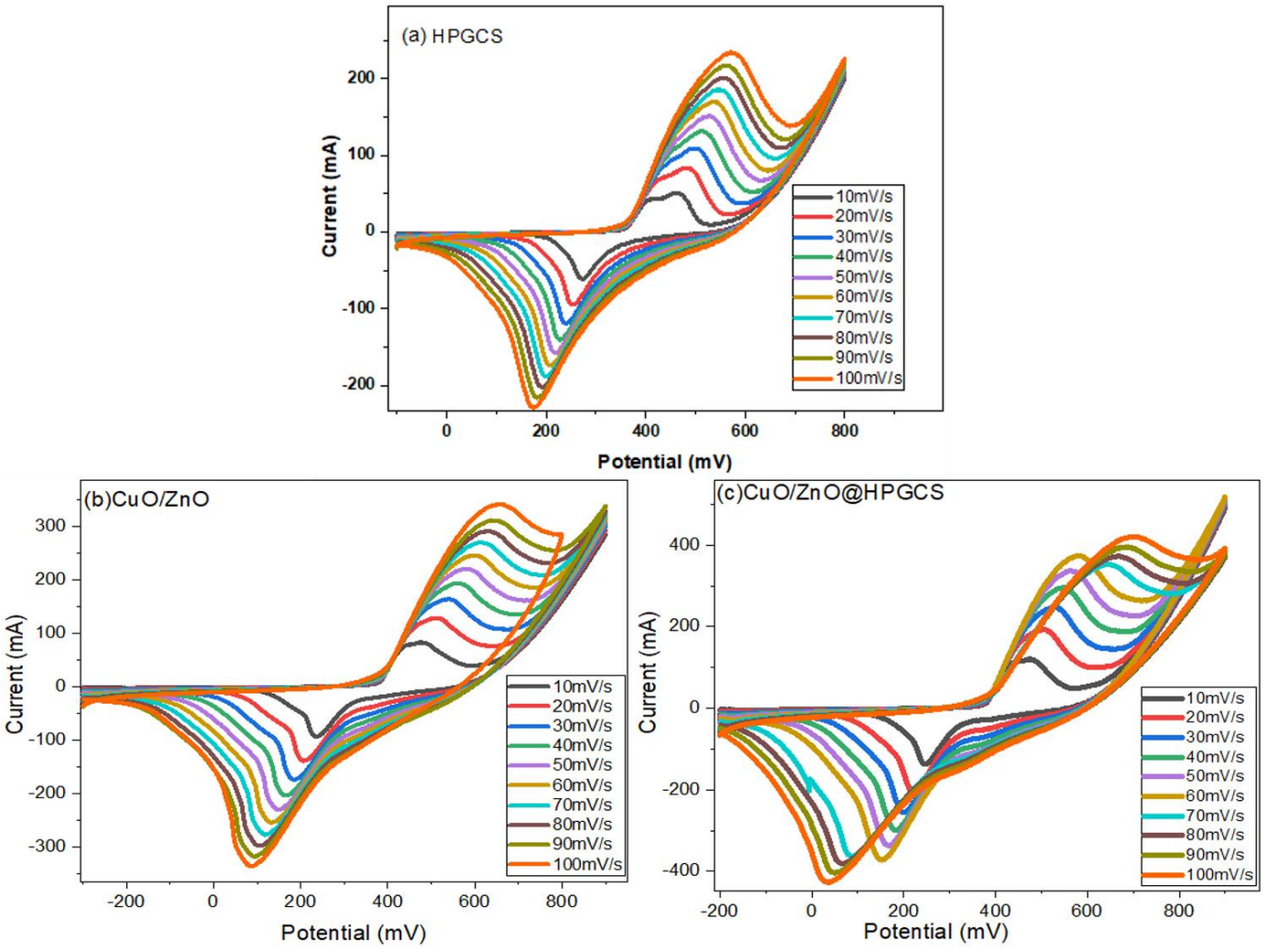


Fig. 4. Electrochemical performance of HPGCS, CuO/ZnO and CuO/ZnO@HPGCS based Ni foam electrode in 3M KOH electrolyte. CV curves at different scan rates from 10-100mV/s (a, b, and c).

© Ariston Publications 2025. All rights reserved.

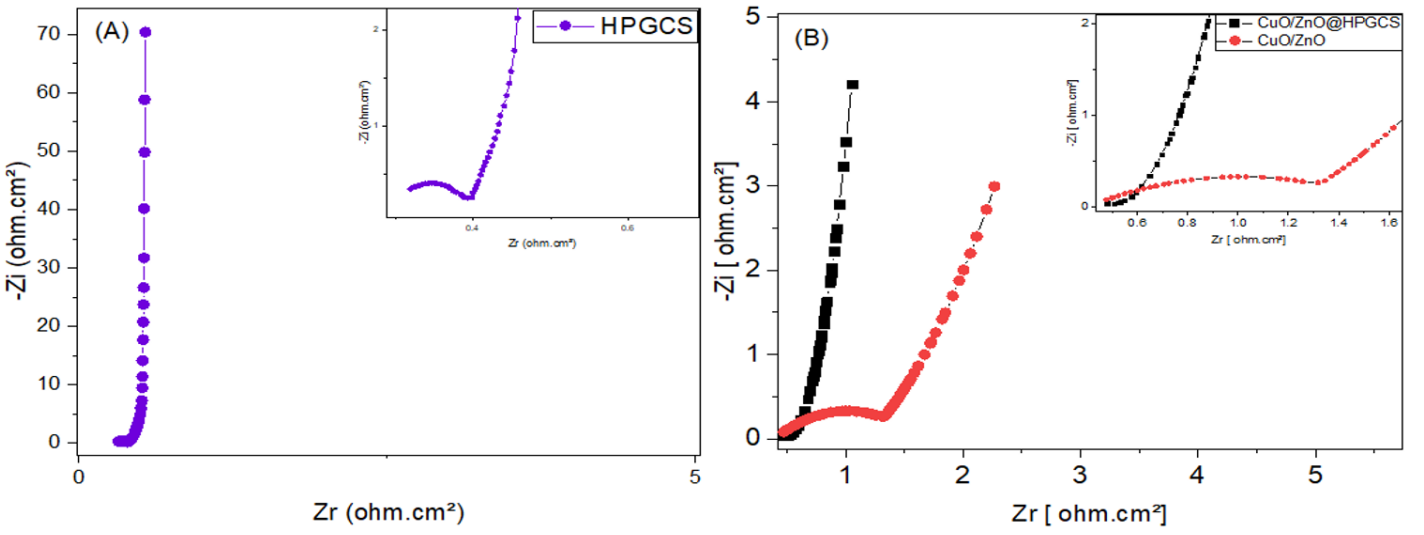


Fig. 5. Nyquist plot of HPGCS, CuO/ZnO and CuO/ZnO@HPGCS based Ni foam electrode in 3M KOH electrolyte. An enlarged depiction of the high frequency portion of the impedance spectra can be seen in the inset.

Whereas linear characteristics were shown in the low frequency zone as shown in figure. In case of HPGCS and CuO/ZnO a small semicircle at higher frequency observed, whereas linear characteristics were shown in lower frequency zone as shown in figure. The almost linear peak, with a slope in the low-frequency range of about 90 denotes capacitive behaviour upon electrode polarization with rapid charge carrier diffusion (high electronic conductivity. Due to the addition of carbonaceous material, the CuO/ZnO@HPGCS composite revealed a high electronic conductivity, and fast charge transfer rate, thereby significantly enhanced electrochemical behavior.

The Nyquist plots' intercept with the actual impedance (Z'), which includes the electrical contact resistance at interface among the active material and the current collector, as well as the material's inherent resistance, and the resistance of the electrolyte, has the ability to calculate the electrode's equivalent series resistance (ESR) (Figure 5 (B)). Nyquist graph can be broken down into three parts; a semicircle at elevated frequency, an angled part (approximately 45 degrees) at intermediate frequency, and a linear part at lower frequencies. Resistance value (Rs) of 0.31 was observed for HPGCS, while 0.46 ohm was observed for CuO/ZnO@HPGCS and 0.47 ohm was observed for CuO/ZnO,at high frequencies, the impedance plots intersection with the real axis reveal the resistive contributions from the electrolyte, active material, and active material- electrolyte interface . Better electrode conductivity is correlated with a lower value of Rs. CuO/ZnO@HPGCS showed less resistance value than CuO/ZnO and HPGCS, indicating better electrode conductivity.

3.4.3. Specific capacitance of all the synthesized nanocomposites

The specific capacitance of all the synthesized nanocomposites was evaluated and compared under varying scan rates, as shown in Figure 6(a). The analysis was performed in a 3 M KOH aqueous electrolyte, which served as the electrolyte medium to examine the electrochemical behavior. All the synthesized materials, including those with and without carbon spheres, demonstrated excellent cyclic stability and promising capacitance performance, making them suitable candidates for energy storage applications.

The ZnO/CuO@HPGCS nanocomposite emerged as the top-performing material, exhibiting a remarkable specific capacitance of 1875 F/g at a scan rate of 10 mV/s. This significant enhancement in capacitance is attributed to the synergistic effects of the hierarchical porous graphitic carbon spheres (HPGCS) and the metal oxides (CuO and ZnO). The incorporation of HPGCS not only provided a high surface area but also facilitated the formation of interconnected three-dimensional porous structures. These structures promoted better ion diffusion and enhanced electron transfer during the charge-discharge cycles, which is critical for achieving superior supercapacitive performance.

In contrast, the composites without carbon spheres exhibited comparatively lower capacitance values, indicating the crucial role of carbon spheres in improving electrochemical properties. The bar chart in Figure 6(b) highlights the capacitance values of all the synthesized materials, clearly illustrating the significant improvement achieved with the ZnO/CuO@HPGCS nanocomposite. The outstanding performance of ZnO/CuO@HPGCS is also attributed to the improved electrical conductivity and reduced resistivity of the composite. The presence of HPGCS ensures a continuous electron pathway, while the CuO and ZnO nanoparticles contribute to the pseudocapacitive behavior by providing active redox sites. Additionally, the porous architecture of the composite enhances electrolyte accessibility, further improving the charge storage capacity.

 © Ariston Publications 2024. All rights reserved

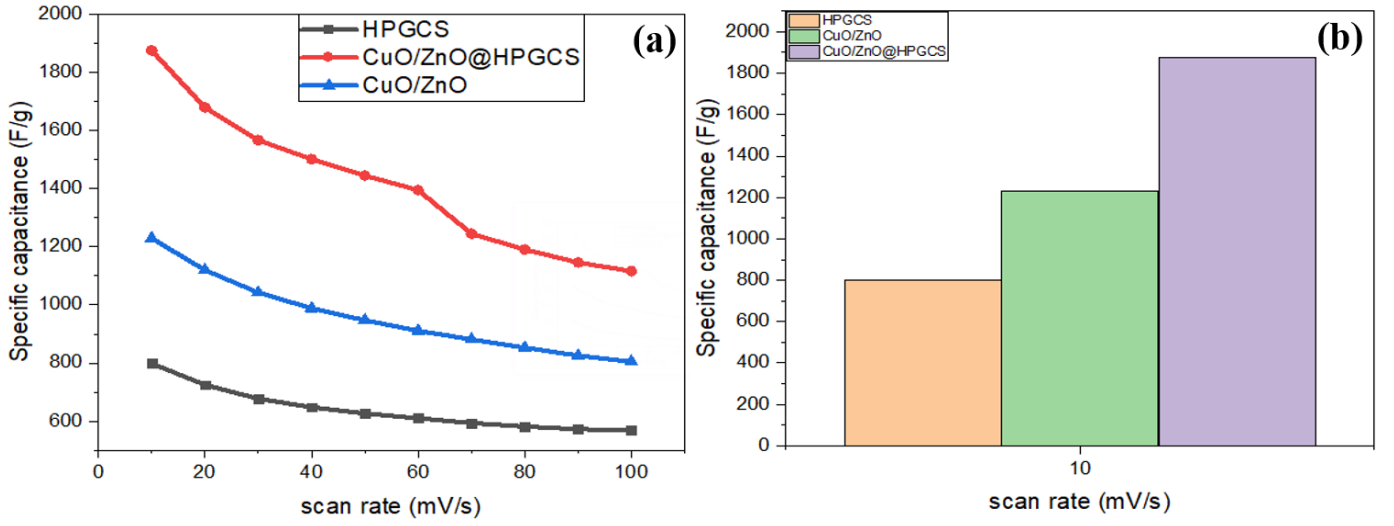


Fig. 6. (a) Specific capacitance of all the synthesized materials in 3 M KOH aqueous electrolyte at different scan rates, (b) Comparison of the specific capacitance of all synthesized material.

The results demonstrate the superior electrochemical performance of ZnO/CuO@HPGCS compared to other synthesized materials. This study emphasizes the importance of integrating hierarchical porous carbon spheres with transition metal oxides to develop advanced materials for next-generation supercapacitor applications. The combination of high capacitance, stability, and scalability makes ZnO/CuO@HPGCS a promising candidate for industrial-scale energy storage solutions.

4. CONCLUSION

The synthesis of CuO/ZnO@hierarchical porous graphitic carbon spheres (CuO/ZnO@HPGCS) demonstrates a promising pathway for developing high-performance supercapacitor materials. The use of chitosan as a low-cost and adaptable precursor during high-temperature carbonization enabled the formation of well-structured porous graphitic carbon spheres (HPGCS). PVP and PEG served as stabilizing agents, ensuring the integrity of the pore structure and facilitating uniform incorporation of CuO/ZnO metal oxides. The fabrication method utilized a simple, low-temperature water-bath technique, avoiding additional annealing treatments, which highlights the method's cost-effectiveness and scalability. Electrochemical evaluation revealed the superior performance of CuO/ZnO@HPGCS electrodes compared to CuO/ZnO and HPGCS alone. The specific capacitance of CuO/ZnO@HPGCS reached 1875 F/g at a scan rate of 10 mV/s, surpassing the performance of CuO/ZnO (1229 F/g) and HPGCS (798 F/g). The nanocomposite exhibited excellent electrical conductivity, reduced resistivity, and a porous architecture that provided abundant active sites, which collectively enhanced charge storage and transfer capabilities. This study underscores the critical role of hierarchical porous carbon materials in improving the electrochemical performance of transition metal oxide-based supercapacitors. The synergistic interaction between CuO/ZnO and HPGCS ensures superior energy storage performance, making this composite highly suitable for next-generation energy storage devices. Overall, CuO/ZnO@HPGCS emerges as an advanced electroactive material for supercapacitor applications due to its excellent energy storage properties, cost-effectiveness, and simple fabrication process. Its scalable production potential makes it a strong candidate for industrial applications aimed at addressing future energy demands. Further studies may focus on optimizing the synthesis parameters and exploring the composite's long-term stability under real-world conditions.

DECLARATIONS

Ethical Approval

We affirm that this manuscript is an original work, has not been previously published, and is not currently under consideration for publication in any other journal or conference proceedings. All authors have reviewed and approved the manuscript, and the order of authorship has been mutually agreed upon.

Funding

Not applicable

Availability of data and material

All of the data obtained or analyzed during this study is included in the report that was submitted.

© Ariston Publications 2025. All rights reserved.

Conflicts of Interest

The authors declare that they have no financial or personal interests that could have influenced the research and findings presented in this paper. The authors alone are responsible for the content and writing of this article.

Authors' contributions

All authors contributed equally in the preparation of this manuscript.

ACKNOWLEDGEMENTS

Authors are highly thankful to The Government Sadiq College Women University (GSCWU), Bahawalpur, Pakistan for financial support.

REFERENCES

[1] Mensah-Darkwa, K., Zequine, C., Kahol, P.K. and Gupta, R.K., **2019.** Supercapacitor energy storage device using biowastes: A sustainable approach to green energy. *Sustainability*, *11*(2), p.414. doi: 10.3390/su11020414.

[2] Nayak, A., Bhushan, B., Kotnala, S., Kukretee, N., Chaudhary, P., Tripathy, A.R., Ghai, K. and Mudliar, S.L., **2023.** Nanomaterials for supercapacitors as energy storage application: Focus on its characteristics and limitations. *Materials Today: Proceedings*, *73*, pp.227-232. doi: 10.1016/j.matpr.2022.11.259.

[3] Shaheen, I., Hussain, I., Zahra, T., Javed, M.S., Shah, S.S.A., Khan, K., Hanif, M.B., Assiri, M.A., Said, Z., Arifeen, W.U. and Akkinepally, B., **2023.** Recent advancements in metal oxides for energy storage materials: design, classification, and electrodes configuration of supercapacitor. *Journal of Energy Storage*, *72*, p.108719. doi: 10.1016/j.est.2023.108719.

[4] Cheng, J., Liu, Y., Zhang, X., Miao, X., Chen, Y., Chen, S., Lin, J. and Zhang, Y., **2021.** Structure engineering in interconnected porous hollow carbon spheres with superior rate capability for supercapacitors and lithium-sulfur batteries. *Chemical Engineering Journal*, *419*, p.129649.doi: 10.1016/j.cej.2021.129649.

[5] Zardkhoshoui, A.M. and Davarani, S.S.H., **2020.** Construction of complex copper-cobalt selenide hollow structures as an attractive battery-type electrode material for hybrid supercapacitors. *Chemical Engineering Journal*, *402*, p.126241.doi: 10.1016/j.cej.2020.126241.

[6] Jose, S. and Varghese, A., **2023.** Design and structural characteristics of conducting polymer-metal organic framework composites for energy storage devices. *Synthetic Metals*, *297*, p.117421. doi: 10.1016/j.synthmet.2023.117421.

[7] Prasankumar, T., Kang, D.J., Kim, M. and Lim, H.T., **2023**. Facile synthesis of flower-like Cu–Zn bimetallic electrodes for high-performance supercapacitors. *International Journal of Electrochemical Science*, *18*(10), p.100315. doi: 10.1016/j.ijoes.2023.100315.

[8] Senthil, R.A., Min, A., Theerthagiri, J., Kim, G.A., Choi, H.C. and Choi, M.Y., **2023.** Insights on Ni-based layered double hydroxides for electrochemical supercapacitors: Underlying aspects in rational design and structural evolution. *Journal of Energy Storage*, *72*, p.108305. doi: 10.1016/j.est.2023.108305.

[9] Kulkarni, A.A., Gaikwad, N.K., Salunkhe, A.P., Dahotre, R.M. and Bhat, T.S., **2023.** Transition metal phosphates: a paradigm for electrochemical supercapacitors. *Journal of Electroanalytical Chemistry*, p.117795. doi: 10.1016/j.jelechem.2023.117795.

[10] Iram, F., Mustafa, G.M., Ali, G., Ahmad, H., Ramay, S.M., Iqbal, Z. and Atiq, S., **2023.** Transition metal (Zn, Mn, and Ni) incorporated CuO nanostructures for supercapacitor applications. *Journal of Energy Storage*, *73*, p.108829. doi: 10.1016/j.est.2023.108829.

[11] Tang, H., Miao, Y., Hu, Z., Ma, L., Sui, Y., Qi, J., Wei, F., Zhang, W., Cao, P., Dang, F. and Sun, Z., **2023.** Design of in-situ grown copper-based bimetallic phosphide electrode materials for efficient energy storage. *Journal of Energy Storage*, *59*, p.106398. doi: 10.1016/j.est.2022.106398.

[12] Pullanchiyodan, A., Joy, R., Sreeram, P., Raphael, L.R., Das, A., Balakrishnan, N.T., Ahn, J.H., Vlad, A., Sreejith, S. and Raghavan, P., **2023.** Recent advances in electrospun fibers based on transition metal oxides for supercapacitor applications: a review. *Energy Advances*, *2*(7), pp.922-947. doi: 10.1039/d3ya00067b.

[13] Sheng, Z., Lin, X., Gao, H., Huang, L., Zhang, Y., Zhao, Y., Wei, H., Wang, C., Xu, D. and Wang, Y., **2022.** Synthesis of hollow carbon-incorporated NiCoM (M= Mn, Cu, Zn) layered double hydroxide nanocages for hybrid supercapacitors. *International Journal of Hydrogen Energy*, *47*(68), pp.29195-29206. doi: 10.1016/j.ijhydene.2022.06.246.

 © Ariston Publications 2024. All rights reserved

[14] Guo, F., Jiang, X., Jia, X., Liang, S., Qian, L. and Rao, Z., **2019.** Synthesis of biomass carbon electrode materials by bimetallic activation for the application in supercapacitors. *Journal of Electroanalytical Chemistry*, *844*, pp.105-115. doi: 10.1016/j.jelechem.2019.05.004.

[15] Moorthi, K. and Mohan, S., **2024.** Developments in Sustainable Green Supercapacitors: A Minireview. *Energy & Fuels*, *38*(23), pp.22719-22745. Doi: https://doi.org/10.1021/acs.energyfuels.4c04548.

[16] Zheng, S.Q., Lim, S.S., Foo, C.Y., Haw, C.Y., Chiu, W.S., Chia, C.H. and Khiew, P.S., **2023.** A novel MOF-derived binary metal oxides and carbon nanocomposite for high-performance symmetric supercapacitor application. *Journal of Materials Science: Materials in Electronics*, *34*(21), p.1578. doi: 10.1007/s10854-023-10976-9.

[17] Rattanaveeranon, S. and Jiamwattanapong, K**., 2022.** Effect of CuO/rGO and ZnO/rGO Hybrid Additional Layers on Supercapacitor Performance. *Trends in Sciences*, *19*(15), pp.5603-5603. doi: 10.48048/tis.2022.5603.

[18] Bishwakarma, H., Kumar Das, A., Kumar, P., Kumar Singh, P. and Awad, M.M., **2023.** Structure and electrochemical properties of CuO-ZnO nanocomposite produced by the one-step novel discharge process. *Journal of Taibah University for Science*, *17*(1), p.2188017. doi: 10.1080/16583655.2023.2188017.

[19] BaQais, A., Alam, M.W., Farhan, M., Muteeb, G., Allag, N. and Mushtaq, S., **2023.** Probe-sonicated synthesis of CuO–ZnO hybrid nanocomposite for photocatalytic and supercapacitor applications. *Inorganics*, *11*(9), p.370. doi: 10.3390/inorganics11090370.

[20] Wen, F., Yan, Y., Sun, S., Li, X., He, X., Meng, Q., Liu, J.Z., Qiu, X. and Zhang, W., **2023.** Synergistic effect of nitrogen and oxygen dopants in 3D hierarchical porous carbon cathodes for ultra-fast zinc ion hybrid supercapacitors. *Journal of Colloid and Interface Science*, *640*, pp.1029-1039. doi: 10.1016/j.jcis.2023.03.024.

[21] Zhang, Z., Lu, S., Li, Y., Song, J., Han, E., Wang, H. and He, Y., **2023.** Promoting hierarchical porous carbon derived from Bamboo via copper doping for high-performance supercapacitors. *Industrial Crops and Products*, *203*, p.117155. doi: 10.1016/j.indcrop.2023.117155.

[22] Ba, Y., Pan, W., Pi, S., Zhao, Y. and Mi, L., **2018.** Nitrogen-doped hierarchical porous carbon derived from a chitosan/polyethylene glycol blend for high performance supercapacitors. *RSC Advances*, *8*(13), pp.7072-7079. doi: 10.1039/c8ra00016f.

[23] Shinde, R.S., More, R.A., Adole, V.A., Koli, P.B., Pawar, T.B., Jagdale, B.S., Desale, B.S. and Sarnikar, Y.P., **2021.** Design, fabrication, antitubercular, antibacterial, antifungal and antioxidant study of silver doped ZnO and CuO nano candidates: A comparative pharmacological study. *Current Research in Green and Sustainable Chemistry*, *4*, p.100138. doi: 10.1016/j.crgsc.2021.100138.

© Ariston Publications 2025. All rights reserved.